JOURNAL OF CHEMICAL EDUCATION

Laboratory Experiment

pubs.acs.org/jchemeduc

Synthesis of Hollow Gold–Silver Alloyed Nanoparticles: A "Galvanic Replacement" Experiment for Chemistry and Engineering Students

Samir V. Jenkins, Taylor D. Gohman, Emily K. Miller, and Jingyi Chen*

Department of Chemistry and Biochemistry, University of Arkansas, Fayetteville, Arkansas 72701, United States

Supporting Information

ABSTRACT: The rapid academic and industrial development of nanotechnology has led to its implementation in laboratory teaching for undergraduate-level chemistry and engineering students. This laboratory experiment introduces the galvanic replacement reaction for synthesis of hollow metal nanoparticles and investigates the optical properties of these nanoparticles. Changes of localized surface plasmon resonance from solid to hollow nanoparticles are monitored by UV–vis spectroscopy, while corresponding morphological changes are validated by transmission electron microscopy. The optical properties are further investigated by the use of a laser pointer, laser irradiation, and surface-enhanced Raman spectroscopy. By performing these experiments, students gain practical knowledge for the synthesis of hollow metal nanoparticles and the underlying structure-dependent optical properties.

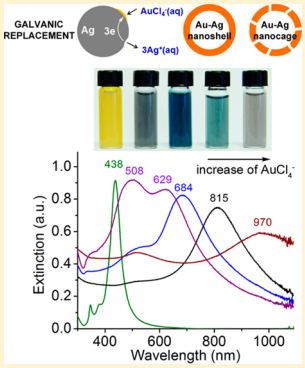

KEYWORDS: *Upper-Division Undergraduate, Interdisciplinary/Multidisciplinary, Nanotechnology, Solid State Chemistry, Colloids, UV–Vis Spectroscopy, Raman Spectroscopy*

INTRODUCTION

Nanoscience and nanotechnology have great potential for significant scientific and industrial advances. Since 2001, the cumulative investment for the National Nanotechnology Initiative has reached $21 billion.[1] Products incorporating nanotechnology made up a market share of $250 billion worldwide in 2009 and were projected to exceed $3 trillion by 2020.[2] To prepare students to join the nanotechnology workforce, there is a growing need to incorporate its frontiers into the chemistry and engineering curricula, particularly laboratory teaching.[3] This laboratory experiment aims to introduce students to an advanced "bottom-up" synthesis method, galvanic replacement, for the preparation of hollow, gold–silver nanoparticles (hAuAgNPs). In this context, students also gain knowledge of optical properties of metal nanoparticles and learn the importance of shape-controlled synthesis.

Noble metal nanoparticles have been extensively investigated in diverse applications, particularly sensing and biomedicine.[4] Most of these applications utilize the unique plasmonic properties of metal nanoparticles, especially those made of gold and silver.[5] The plasmonic properties, known as localized surface plasmon resonance (LSPR), arise from the collective oscillation of the conduction electrons within a metal nanoparticle in response to incident light at their resonance frequency. The LSPR is the sum of light scattering and absorption. One can tailor the plasmonic properties by manipulating the composition and morphology of the nanoparticles to facilitate the corresponding applications.[6]

A growing number of undergraduate-level experiments that use gold and silver nanoparticles (AuNPs and AgNPs, respectively) have been introduced to laboratory teaching. An early example demonstrated AuNP synthesis through reduction of Au precursors with citrate ions and used these AuNPs as a colorimetric ion detector.[7] A synthesis module introduced a "green" chemical route to generate AuNPs using tea leaves.[8] The optical properties of these nanoparticles were further explored in several laboratory experiments: AuNPs were incorporated into polymers to emulate stained glass;[9] enzyme-induced growth of AuNPs was used to sense glucose;[10] and AgNPs were used as substrates to enhance Raman scattering of molecules.[11] A recent laboratory experiment demonstrated the synthesis of Ag nanoprisms and investigated their size-dependent optical properties.[12] In the context of shape-controlled synthesis, we introduce a galvanic replacement at the nanoscale to synthesize hollow metal nanostructures with well-defined morphology.

Hollow metal nanostructures are advantageous over their solid counterparts because of their more finely tunable optical properties and larger surface area.[13,14] They are under intense investigation for biomedicine and catalysis.[15−17] The galvanic replacement reaction is a versatile method to produce hollow nanostructures from a solid template.[18,19] The laboratory experiment described here introduces students to the galvanic replacement between solid Ag nanocubes (AgNCs) and $HAuCl_4$ to form hollow Au–Ag alloyed nanoparticles (hAuAgNPs). The optical properties of these nanostructures

Published: March 18, 2015

DOI: 10.1021/acs.jchemed.5b00042
J. Chem. Educ. 2015, 92, 1056–1060

are further investigated by UV−vis spectroscopy, photothermal conversion, and surface-enhanced Raman spectroscopy (SERS). This laboratory consolidates a deeper comprehension of the underlying synthetic mechanism and structure−function relationship of hollow metal nanostructures.

EXPERIMENTAL OVERVIEW

Upper-level undergraduate and graduate students of chemistry or engineering are introduced to the galvanic replacement reaction for the production of hAuAgNPs. The laboratory experiment has been implemented as a module consisting of four 2-h periods within a nanotechnology laboratory course. The approximate timetable for experiments is included in Table 1. The first period is a lecture that provides students with background knowledge. The second and third periods are devoted to laboratory experiments. Students are assembled into small working groups of 2−3 for the duration of the experiment. The fourth period is organized as group discussion wherein students present their results to the class in the form of a short slideshow. Full experimental details are included in the Supporting Information.

Table 1. Summary of Activities in the Laboratory

Period	Activities	Time Required
1	Lecture of metal nanostructures and plasmonics	2 h
2	Galvanic replacement to form hAuAgNPs	2 h
3	Investigation of optical properties	1 h
	Demonstration of photothermal effect and SERS	1 h
4	Group presentation	2 h

CHEMICALS

All chemicals were used as received (see Supporting Information). Experiments were performed using deionized H_2O with resistivity of 18 MΩ. Stock solutions were prepared by the teaching assistant prior to the class (see Notes for Instructors in the Supporting Information).

HAZARDS

The biosafety of metal nanoparticles is not fully understood. Because $HAuCl_4$ stains skin upon contact, gloves should be worn when handling these chemicals and materials. Lasers can cause severe eye damage and should never be pointed toward an individual. Personal protective equipment such as lab coat, gloves, and safety glasses should be worn during the synthesis component of the lab. Glassware should be cleaned with aqua regia, which is highly corrosive, and should only be used with caution in a fume hood and safely neutralized after completion of the lab.

GALVANIC REPLACEMENT

Galvanic replacement is a single displacement reaction driven by the electrochemical potential difference between two reactants; hAuAgNPs can be synthesized by the galvanic replacement between AgNCs and $HAuCl_4$ following eq 1:

$$3Ag(s) + AuCl_4^-(aq) \xrightarrow{heat} Au(s) + 3Ag^+(aq) + 4Cl^-(aq) \quad (1)$$

AgNCs used in the galvanic replacement are synthesized by the teaching assistant using the polyol method prior to the experiment periods. The AgNC serves as both a sacrificial template and an anode (E^o_{Ag/Ag^+} = 0.799 V) in the reaction. Ag^0 is oxidized and dissolved as Ag^+, while Au^{3+} is reduced to Au^0 ($E^o_{Au/[AuCl_4]^-}$ = 0.930 V) and subsequently plates on the surface of the AgNCs (Figure 1). The standard electrochemical

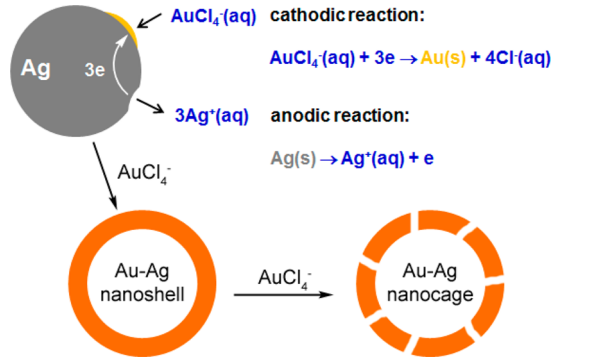

Figure 1. Schematic illustration of the synthesis of hAuAgNPs via galvanic replacement reaction between AgNCs and $HAuCl_4$.

difference between $E^o_{Ag/Ag+}$ (0.799 V) and $E^o_{Ag/AgCl}$ (0.222 V) is attributed to the coupling of equilibrium, $AgCl(s) \leftrightarrow Ag^+(aq) + Cl^-(aq)$, to the Ag/Ag^+ half reaction. To prevent the precipitation of AgCl(s) during the galvanic replacement, the reaction is maintained at the boiling temperature of water ensuring the concentration of Ag^+ and Cl^- ions below the solubility product constant (K_{sp}).[20] Therefore, Ag^+ ion remains dissolved during the reaction. After the reaction, AgCl(s) precipitates out of the solution upon cooling, observable as white precipitate at the bottom of the flask.

Diffusion occurs across the interface between Au and Ag to form alloyed Au−Ag. As more $HAuCl_4$ is reduced, the particle interior is gradually emptied, which forms the hAuAgNPs. As the stoichiometry involves displacement of three Ag by one Au, the total number of atoms per particle decreases. Thus, the morphology of hAuAgNPs changes from nanoshell to nanocage during the course of the replacement reaction. The morphology of AgNCs and hAuAgNPs is characterized by transmission electron microscopy (TEM). The TEM images are acquired by a teaching assistant, and size analysis is then performed by the students using ImageJ software (NIH). In this laboratory, each group applies different amounts of Au to react with the same amount of AgNCs to yield morphologically and optically distinct hAuAgNPs for comparison in the group discussion.

OPTICAL PROPERTIES

The LSPR of metal nanoparticles results in strong light absorption and scattering at the resonance wavelength. The extinction of AgNCs and hAuAgNPs is characterized using a UV−vis spectrometer. For AgNCs, the LSPR maximum (λ_{max}, nm) shifts slightly to the red as the particle size increases. This relationship was empirically described by Xia and co-workers using eq 2:[21]

$$\lambda_{max} = 1.3927(l) + 378.25 \quad (2)$$

where l is the edge length (nm) of the AgNCs measured from TEM images. As the galvanic replacement proceeds, the peak gradually shifts from the visible to the near-infrared region. The peak shifts are recorded with a UV−vis spectrometer. The absorption and scattering components of the LSPR are qualitatively investigated with a laser pointer.

DOI: 10.1021/acs.jchemed.5b00042
J. Chem. Educ. 2015, 92, 1056−1060

Metal nanoparticles can convert photon energy into thermal energy, known as the photothermal effect. The efficiency of light-to-heat conversion is proportional to the absorption efficiency of the nanoparticles. The temperature increase depends on not only the concentration and spectral profile of the nanoparticles, but also the light dose. The time-dependent temperature profile can be described by eqs 3 and 4:

$$T(t) = T_0 + A/B(1 - e^{-Bt}) \qquad \text{Laser on} \qquad (3)$$

$$T(t) = T_0 + (T_{max} - T_0)e^{-Bt} \qquad \text{Laser off} \qquad (4)$$

where $T(t)$ is the temperature at a particular time, T_0 is the starting temperature, and T_{max} is the temperature when irradiation is removed, all in °C. A is the rate of energy absorption (°C/s), and B is the rate constant of heat dissipation (s^{-1}).[22] B is initially calculated by fitting the data from the profile after irradiation to eq 4 and then used to determine the value for A during irradiation by fitting to eq 3. In the demonstration, the temperature is monitored by a thermocouple, and the results for different samples are compared.

The LSPR can enhance the Raman signal of molecules adsorbed on or in close proximity to a nanoparticle surface, a phenomenon known as SERS. A metal nanoparticle acts as a two-way antenna by increasing incident light flux and amplifying the scattered Raman signal, which results in quartic enhancement (E^4).[23] SERS enhancement can be compared quantitatively by enhancement factor (EF) for individual particles in solution or on substrates.[24−26] From the SERS substrate point of view, the average EF defined in eq 5 is the most widely used:[27]

$$EF = \frac{I_{SERS}/N_{Surf}}{I_{RS}/N_{Vol}} \qquad (5)$$

where I_{SERS} is the intensity of a Raman active mode observed in the SERS sample, I_{RS} is the intensity of the same mode detected in the reference, N_{Surf} is the average number of adsorbed molecules in the scattering volume for the SERS experiment, and N_{Vol} is the average number of molecules in the scattering volume for the Raman (non-SERS) measurement. From the analytical chemistry point of view, the analytical enhancement factor (AEF) is defined in eq 6:[27]

$$AEF = \frac{I_{SERS}/C_{SERS}}{I_{RS}/C_{RS}} \qquad (6)$$

where C_{SERS} is the concentration of molecules adsorbed on the SERS substrate, and C_{RS} is the concentration of molecules in the reference. If monolayer coverage on the surface is ensured, the AEF is a simplified form of the EF in eq 5 and frequently used for colloidal solutions.[27] In this experiment, the AEF values of different samples have been derived and compared.

RESULTS AND DISSCUSSION

Transmission Electron Microscopy and UV−vis Spectroscopy Characterization

The galvanic replacement reaction occurs between the AgNCs and $HAuCl_4$ in aqueous solution. The AgNCs were prepared by the polyol method as described in the Supporting Information.[21] They had edge lengths of 46.6 ± 5.3 nm and an LSPR maximum of 438 nm (Figure 2A). Using eq 2, the edge length was predicted to be 42.9 nm, which is close to the measured value. Discrepancies can be attributed to the presence of small quantities of other morphologies in the sample, along with variations among particles selected for size measurement from the TEM image.

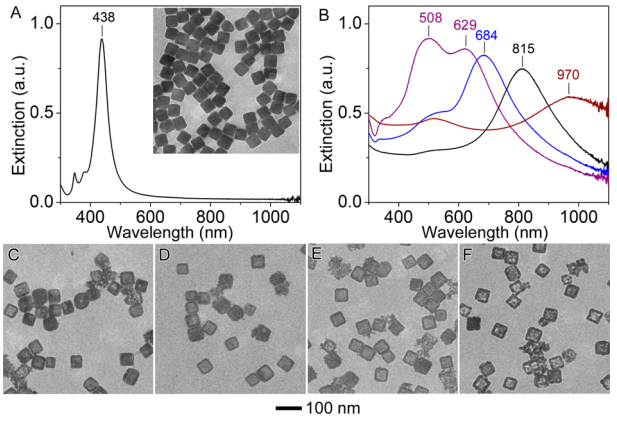

Figure 2. Characterization of nanoparticles used and synthesized during this module: (A) extinction spectrum and inset TEM image of AgNCs used as sacrificial template; (B) extinction spectra corresponding to addition of 3 mL (purple), 4 mL (blue), 5 mL (black), or 6 mL (wine) of 1 mM $HAuCl_4$; and (C−F) TEM images of the samples corresponding to addition of 3, 4, 5, or 6 mL of 1 mM $HAuCl_4$.

The AgNCs were then used as sacrificial templates for the galvanic replacement reaction to yield hAuAgNPs.[20] The morphological and compositional changes of nanoparticles led to the progressive red-shift of LSPR (Figure 2B−F). The addition of a small amount of Au initially leads to the formation of pits on the Ag surface. Further titration of Au^{3+} leads to dissolution of the Ag in the particle interior to form hAuAgNPs. As the volume of 1 mM $HAuCl_4$ is increased from 3 to 4, 5, and 6 mL, the LSPR shifts from a dual-band peak at 508 and 629 nm, to single peaks at 684, 815, and 970 nm, respectively.

The spectral changes depend on the concentration ratio of AgNCs and $HAuCl_4$. Therefore, some variation in the final spectrum relative to the amount of $HAuCl_4$ titrated is expected. Generally, the wavelength range can be visualized by a color progression from royal blue (~665 nm) to navy blue (~700−800 nm) and then grayish black (>800 nm) as the amount of $HAuCl_4$ titrant increases with a fixed number of AgNCs.

Absorption and Scattering Characterization

To further illustrate the light absorption and scattering of the metal nanoparticles, the beam emitted from a red laser pointer is passed through samples of H_2O, 100 mM $CuSO_4$, AgNCs, and hAuAgNPs (Figure 3). The beam is visible as a result of scattering. Neither H_2O nor $CuSO_4$ show appreciable scattering of the laser. The AgNCs show a cylindrical beam without significant tapering, which indicates that scattering is the primary process. In contrast, the hAuAgNPs, particularly those overlapping with the laser wavelength, show substantial reduction of the beam size due to the relatively strong absorption component of the LSPR. These effects are visible under room lighting but are significantly more pronounced in the dark.

Photothermal Conversion

The photothermal effect was investigated using an NIR laser at 808 nm with power density of 0.5 W/cm^2 for 5 min. During irradiation, the temperature profile was recorded (Figure 4). The AgNC and H_2O samples do not significantly change temperature due to low absorption at the irradiation wavelength. The temperature of the $CuSO_4$ and hAuAgNP samples

DOI: 10.1021/acs.jchemed.5b00042
J. Chem. Educ. 2015, 92, 1056−1060

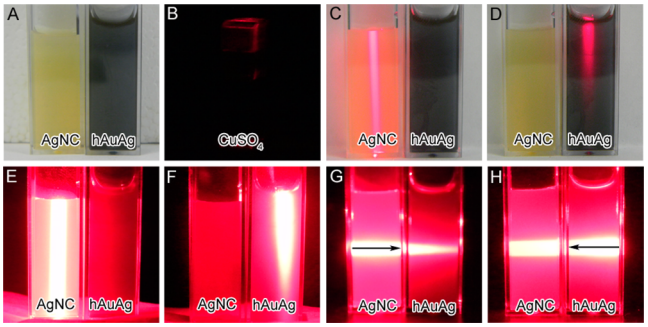

Figure 3. Photographs of interactions of various samples with a 650 nm laser pointer: (A) no irradiation; (B) downward irradiation of $CuSO_4$ in the dark; (C, D) downward irradiation under ambient lighting; (E, F) downward irradiation in the dark; (G) irradiation from the AgNC side; and (H) irradiation from the hAuAgNP side.

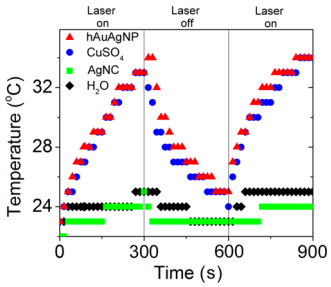

Figure 4. Temperature profile for solutions of hAuAgNPs (red), $CuSO_4$ (blue), AgNCs (green), and H_2O (black) under 5 min cycles with and without irradiation by 808 nm diode laser.

(0.01 nM) rises and falls by roughly 10 °C during these cycles. By fitting eqs 3 and 4, the rate of energy absorption (A) and the rate constant of heat dissipation (B) can be derived. For example, a sample of hAuAgNPs resulted in an A value of 0.072 °C/s and a value for B of 0.0061 s^{-1}. These values are expected to vary with the concentration and optical properties of the particles as well as irradiation wavelength and dose.

Surface-Enhanced Raman Spectroscopy

The SERS effect was investigated by comparing Raman signal intensity of 4-mercaptobenzoic acid (4-MBA) in the SERS spectra with that in the Raman (non-SERS) spectrum. Each SERS sample contained 4.5×10^{-6} M 4-MBA adsorbed on 0.1 nM of hAuAgNPs with edge length of 50 nm (~0.9 m^2/L total surface area) assuming that each hAuAgNPs has a nonporous, smooth surface and that the packing density of 4-MBA on Au as a monolayer is ~0.5 nmol/cm^2. The reference sample was 1.0×10^{-2} M 4-MBA in 0.1 M NaOH aqueous solution. The Raman spectra were collected using a 785 nm laser with power of 100 mW and integration time of 30 s in one acquisition (Figure 5). The peaks at 1083 and 1590 cm^{-1} are attributed to the ring-breathing modes ($\nu(CC)_{ring}$) of 4-MBA, while the peak at 1428 cm^{-1} is assigned to a stretching mode of COO^- ($\nu_s(COO^-)$).[23,24,28] The values of AEF calculated using the peak at 1590 cm^{-1} are listed in Table 2. Ideally, the AEF values should average all of the Raman active modes; however, some of the peaks are hardly resolvable due to instrument limitations. The values of AEF for the alloyed hAuAgNPs are on the orders of 10^3–10^4 comparable with that reported in the literature[25] and decrease with increased Au composition. Compared to pure Ag, the alloys increase the stability of the nanoparticles against oxidation.

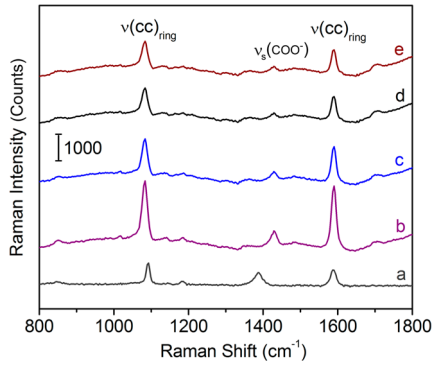

Figure 5. Raman (non-SERS) (a) and SERS spectra (b–e) of 4-mercaptobenzoic acid (4-MBA): (a) 0.010 M 4-MBA in 0.1 M NaOH aqueous solution; (b–e) 4-MBA molecules adsorbed on hAuAgNPs with a total surface area of 0.9 m^2/L synthesized with (b) 3 mL, (c) 4 mL, (d) 5 mL, or (e) 6 mL of 1 mM $HAuCl_4$.

Table 2. Summary of Spectral Properties Derived from Figure 5

Samples	Raman Intensity at 1590 cm^{-1}	AEF
a	700	reference
b	2761	8.7×10^3
c	1591	5.0×10^3
d	1099	3.5×10^3
e	1088	3.4×10^3

FORMATIVE ASSESSMENT

Formative assessment was carried out using a short quiz, group presentation, and laboratory report. A 15 min quiz with five questions was given at the end of period 1. The quiz is designed to provide feedback concerning the lecture and ensure that students understand the experimental background. A sample quiz is provided in the Supporting Information. The group presentation is performed by each student group during period 4. The presentation should include an introduction, results, discussion, and conclusion. To avoid repetition, each group is limited to different introduction topics. Since each group used different amounts of $HAuCl_4$ to titrate the AgNCs, the morphological and spectral changes can be compared across groups. Upon the completion of this laboratory, students are required to write a report using a scientific style.[29] The report allows instructors to assess the students' understanding of the entire laboratory and their scientific writing skills. This laboratory has been integrated into an interdisciplinary nanotechnology laboratory course in fall of 2013 and 2014. The size of the class is 10–12 students, typically juniors and seniors in chemistry, physics, or engineering. On the basis of the formative assessments, students were engaged in the laboratory experiment and performed well. Thirty percent of students conducted research with a professor in nanotechnology, and ~20% of them received a minor in nanotechnology. This laboratory provides students with background and hands-on experience in materials chemistry and nanotechnology to better prepare them for their professional careers.

CONCLUSION

This laboratory introduces students to the aqueous synthesis of hAuAgNPs using a galvanic replacement reaction between AgNCs and varying amounts of $HAuCl_4$. The visible changes in

DOI: 10.1021/acs.jchemed.5b00042
J. Chem. Educ. 2015, 92, 1056–1060

the LSPR during the titration provide a simple and robust means for students to grasp the changes in nanoparticle morphology and optical properties. By varying the amount of titrant in the synthesis among groups, students are able to compare results and establish the correlation between morphology and LSPR. The absorption and scattering components of the LSPR for AgNCs and hAuAgNPs are easily demonstrated using the laser pointer, photothermal, and SERS experiments described. This laboratory will reinforce the learning of optical phenomena and nanochemistry as well as introduce characterization techniques associated with nanomaterial research.

■ ASSOCIATED CONTENT

Supporting Information

Instructor notes, experimental procedures, and student lab handout. This material is available via the Internet at http://pubs.acs.org.

■ AUTHOR INFORMATION

Corresponding Author

*E-mail: chenj@uark.edu.

Notes

The authors declare no competing financial interest.

■ ACKNOWLEDGMENTS

The authors would like to acknowledge the funding support by NSF-NUE (EEC-1138248). We would like to thank M. Zou for leading the laboratory course on nanotechnology, and the students for engaging in the new lab activity. We also thank B. Durham and R. Koeppe for critical review.

■ REFERENCES

(1) *National Nanotechnology Initiative*; U.S. National Nanotechnology Initiative: Washington, DC. www.nano.gov (accessed March 2015).
(2) Roco, M. C. The Long View of Nanotechnology Development: The National Nanotechnology Initiative at 10 Years. *Nanotechnology Research Directions for Societal Needs in 2020*; Springer: New York, 2011; pp 1−28.
(3) Roco, M. C. Converging Science and Technology at the Nanoscale: Opportunities for Education and Training. *Nat. Biotechnol.* **2003**, *21*, 1247−1249.
(4) Jenkins, S. V.; Muldoon, T. J.; Chen, J. Plasmonic Nanostructures for Biomedical and Sensing Applications. *Metallic Nanostructures*; Xiong, Y., Lu, X., Eds.; Springer International Publishing: New York, 2015; pp 133−173.
(5) Xia, Y.; Campbell, D. J. Plasmons: Why Should We Care? *J. Chem. Educ.* **2007**, *84*, 91.
(6) Wilets, K. A.; Duyne, R. P. V. Localized Surface Plasmon Resonance Spectroscopy and Sensing. *Annu. Rev. Phys. Chem.* **2007**, *58*, 267−97.
(7) McFarland, A. D.; Haynes, C. L.; Mirkin, C. A.; Van Duyne, R. P.; Godwin, H. A. Color My Nanoworld. *J. Chem. Educ.* **2004**, *81*, 544A.
(8) Sharma, R. K.; Gulati, S.; Mehta, S. Preparation of Gold Nanoparticles Using Tea: A Green Chemistry Experiment. *J. Chem. Educ.* **2012**, *89*, 1316−1318.
(9) Campbell, D. J.; Villarreal, R. B.; Fitzjarrald, T. J. Take-Home Nanochemistry: Fabrication of a Gold- or Silver-Containing Window Cling. *J. Chem. Educ.* **2012**, *89*, 1312−1315.
(10) Bai, J.; Flowers, K.; Benegal, S.; Calizo, M.; Patel, V.; Bishnoi, S. W. Using the Enzymatic Growth of Nanoparticles To Create a Biosensor. An Undergraduate Quantitative Analysis Experiment. *J. Chem. Educ.* **2009**, *86*, 712.
(11) Pavel, I. E.; Alnajjar, K. S.; Monahan, J. L.; Stahler, A.; Hunter, N. E.; Weaver, K. M.; Baker, J. D.; Meyerhoefer, A. J.; Dolson, D. A. Estimating the Analytical and Surface Enhancement Factors in Surface-Enhanced Raman Scattering (SERS): A Novel Physical Chemistry and Nanotechnology Laboratory Experiment. *J. Chem. Educ.* **2011**, *89*, 286−290.
(12) Frank, A. J.; Cathcart, N.; Maly, K. E.; Kitaev, V. Synthesis of Silver Nanoprisms with Variable Size and Investigation of Their Optical Properties: A First-Year Undergraduate Experiment Exploring Plasmonic Nanoparticles. *J. Chem. Educ.* **2010**, *87*, 1098−1101.
(13) Sun, Y.; Xia, Y. Shape-Controlled Synthesis of Gold and Silver Nanoparticles. *Science* **2002**, *298*, 2176−2179.
(14) González, E.; Arbiol, J.; Puntes, V. F. Carving at the Nanoscale: Sequential Galvanic Exchange and Kirkendall Growth at Room Temperature. *Science* **2011**, *334*, 1377−1380.
(15) Skrabalak, S. E.; Chen, J.; Sun, Y.; Lu, X.; Au, L.; Cobley, C. M.; Xia, Y. Gold Nanocages: Synthesis, Properties, and Applications. *Acc. Chem. Res.* **2008**, *41*, 1587−1595.
(16) Zeng, J.; Zhang, Q.; Chen, J.; Xia, Y. A Comparison Study of the Catalytic Properties of Au-Based Nanocages, Nanoboxes, and Nanoparticles. *Nano Lett.* **2009**, *10*, 30−35.
(17) Chen, J.; Yang, M.; Zhang, Q.; Cho, E. C.; Cobley, C. M.; Kim, C.; Glaus, C.; Wang, L. V.; Welch, M. J.; Xia, Y. Gold Nanocages: A Novel Class of Multifunctional Nanomaterials for Theranostic Applications. *Adv. Funct. Mater.* **2010**, *20*, 3684−3694.
(18) Lu, X.; Chen, J.; Skrabalak, S.; Xia, Y. Galvanic Replacement Reaction: A Simple and Powerful Route to Hollow and Porous Metal Nanostructures. *Proc. Inst. Mech. Eng., Part N* **2007**, *221*, 1−16.
(19) Xia, X.; Wang, Y.; Ruditskiy, A.; Xia, Y. 25th Anniversary Article: Galvanic Replacement: A Simple and Versatile Route to Hollow Nanostructures with Tunable and Well-Controlled Properties. *Adv. Mater.* **2013**, *25*, 6313−6333.
(20) Sun, Y.; Xia, Y. Mechanistic Study on the Replacement Reaction between Silver Nanostructures and Chloroauric Acid in Aqueous Medium. *J. Am. Chem. Soc.* **2004**, *126*, 3892−3901.
(21) Zhang, Q.; Li, W.; Wen, L.-P.; Chen, J.; Xia, Y. Facile Synthesis of Ag Nanocubes of 30 to 70 nm in Edge Length with CF_3COOAg as a Precursor. *Eur. J. Chem.* **2010**, *16*, 10234−10239.
(22) Richardson, H. H.; Carlson, M. T.; Tandler, P. J.; Hernandez, P.; Govorov, A. O. Experimental and Theoretical Studies of Light-to-Heat Conversion and Collective Heating Effects in Metal Nanoparticle Solutions. *Nano Lett.* **2009**, *9*, 1139−1146.
(23) Talley, C. E.; Jackson, J. B.; Oubre, C.; Grady, N. K.; Hollars, C. W.; Lane, S. M.; Huser, T. R.; Nordlander, P.; Halas, N. J. Surface-Enhanced Raman Scattering from Individual Au Nanoparticles and Nanoparticle Dimer Substrates. *Nano Lett.* **2005**, *5*, 1569−1574.
(24) Orendorff, C. J.; Gole, A.; Sau, T. K.; Murphy, C. J. Surface-Enhanced Raman Spectroscopy of Self-Assembled Monolayers: Sandwich Architecture and Nanoparticle Shape Dependence. *Anal. Chem.* **2005**, *77*, 3261−3266.
(25) McLellan, J. M.; Siekkinen, A.; Chen, J.; Xia, Y. Comparison of the Surface-Enhanced Raman Scattering on Sharp and Truncated Silver Nanocubes. *Chem. Phys. Lett.* **2006**, *427*, 122−126.
(26) Hrelescu, C.; Sau, T. K.; Rogach, A. L.; Jäckel, F.; Feldmann, J. Single Gold Nanostars Enhance Raman Scattering. *Appl. Phys. Lett.* **2009**, *94*, 153113.
(27) Le Ru, E.; Blackie, E.; Meyer, M.; Etchegoin, P. G. Surface Enhanced Raman Scattering Enhancement Factors: A Comprehensive Study. *J. Phys. Chem. C* **2007**, *111*, 13794−13803.
(28) Talley, C. E.; Jusinski, L.; Hollars, C. W.; Lane, S. M.; Huser, T. Intracellular pH Sensors Based on Surface-Enhanced Raman Scattering. *Anal. Chem.* **2004**, *76*, 7064−7068.
(29) Garland, C. W.; Nibler, J. W.; Shoemaker, D. P. *Experiments in Physcial Chemistry*, 8th ed.; McGraw-Hill: New York, 2009; pp 13−26.

DOI: 10.1021/acs.jchemed.5b00042
J. Chem. Educ. 2015, 92, 1056−1060